

Magnetic heat pumping near room temperature

Cite as: Journal of Applied Physics **47**, 3673 (1976); <https://doi.org/10.1063/1.323176>
Published Online: 29 August 2008

G. V. Brown



View Online



Export Citation

ARTICLES YOU MAY BE INTERESTED IN

[Giant magnetocaloric effect of \$\text{MnAs}_{1-x}\text{Sb}_x\$](#)

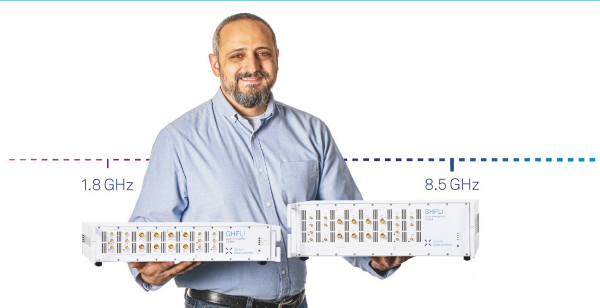
Applied Physics Letters **79**, 3302 (2001); <https://doi.org/10.1063/1.1419048>

[Advanced materials for magnetic cooling: Fundamentals and practical aspects](#)

Applied Physics Reviews **4**, 021305 (2017); <https://doi.org/10.1063/1.4983612>


[Magnetocaloric effect from indirect measurements: Magnetization and heat capacity](#)

Journal of Applied Physics **86**, 565 (1999); <https://doi.org/10.1063/1.370767>



Trailblazers. New

Meet the Lock-in Amplifiers that measure microwaves.

 Zurich Instruments [Find out more](#)

Magnetic heat pumping near room temperature

G. V. Brown

National Aeronautics and Space Administration, Lewis Research Center, Cleveland, Ohio 44135
(Received 15 December 1975)

Magnetic heat pumping can be made practical at room temperature by using a ferromagnetic material with a Curie point in or near the operating temperature range and an appropriate regenerative thermodynamic cycle. Rare earths are found to be much more effective in this application than transition elements, and measurements have been made which show that gadolinium (Curie point: 293°K) is a reasonable working material. The application of a 7-T magnetic field to Gd at the Curie point causes a heat release of 4 kJ/kg under isothermal conditions or a temperature rise of 14°K under adiabatic conditions. A regeneration technique is proposed which removes the limits usually expected on the temperature span of a magnetic cycle. The cycle efficiency can approach the Carnot-cycle efficiency.

PACS numbers: 85.80.Lp, 75.50.Cc, 65.50.+m

INTRODUCTION

For over three decades magnetic heat pumping was possible only within a few degrees of absolute zero. Very dilute hydrated paramagnetic salts of rare earths were generally used as working materials and field strengths were no more than about 2 T. The development of superconducting magnets that produce field strengths of several T made it reasonable to consider cycles running from 4°K up to 15 or 20°K.^{1,2} In this temperature range, more concentrated nonhydrated rare-earth salts can be used. The suitability of a number of such salts has been investigated experimentally.^{1,3-6} The potential of the magnetic cycle for temperatures from 20°K to room temperature has not been studied for two reasons. First, in paramagnetic materials, the degree of magnetic order becomes small at higher temperatures for a 10-T applied field (an approximate maximum practical field strength at the time of this writing) and, hence, the resulting isothermal entropy change becomes small. Second, at 20°K, the lattice entropies of typical salts are comparable to that isothermal entropy change. As shown in Ref. 2, in a simple magnetic cycle the change in lattice entropy between the upper and lower isotherms must be subtracted from the entropy that would otherwise be pumped per cycle. Hence, the refrigeration capacity of all known paramagnetic materials approaches zero for sink temperatures near 20°K or lower if the source temperature is 4°K.

However, neither of these obstacles is absolute. Intuition, theory, and experiment all say that heating and cooling effects in a magnetic material are greatest near a Curie point T_c . The ordering influence of the exchange interaction and the disordering effect of thermal agitation are in approximate balance near T_c . In this neighborhood, applying a field under isothermal conditions produces a greater increase in magnetization (decrease in entropy) than at a higher temperature T where only a paramagnetic response could be produced or at much lower T where the spontaneous magnetization approaches saturation and cannot be increased to any great extent. Similarly, the application of a field under adiabatic conditions gives a temperature change which is sharply peaked near T_c . Edison and Tesla held early patents (1887 and 1890)^{7,8} for a heat engine based on the inverse of this effect. Later papers and patents dis-

cussed the use of the principle for engines⁹⁻¹² and for refrigeration.^{12,13} However, suitable working materials and appropriate thermodynamic cycles have not been suggested for temperatures above 20°K.

Suitable materials do exist even for use at temperatures as high as room temperature. In the element Gd, the isothermal entropy change ΔS due to applying a 7-T field is $0.25R$, where R is the universal gas constant, 8.31 J/mole°K at room temperature. Temperature changes ΔT of 14°K have been produced at room temperature by applying a 7-T field to Gd metal in exploratory experiments in this laboratory. The Curie point of Gd is 293°K¹⁴⁻¹⁶ which makes it a prime candidate for the working material in a room-temperature heat pump.

In this paper, a portion of an entropy temperature diagram for gadolinium is constructed from published

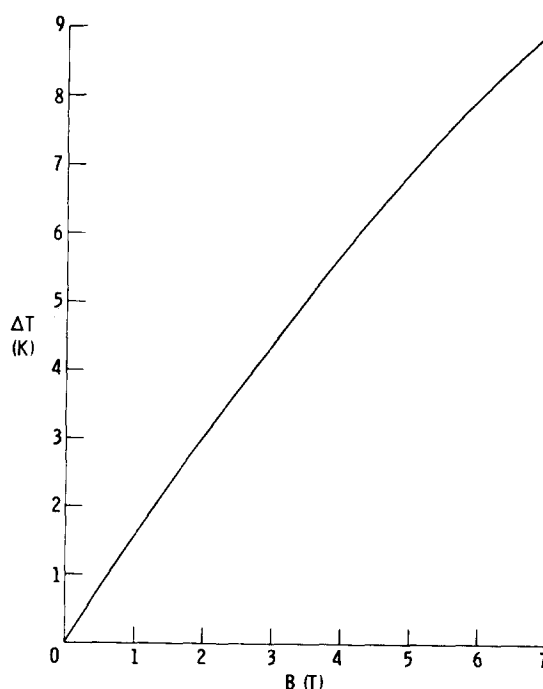


FIG. 1. Adiabatic temperature change ΔT produced by applying field B . Initial temperature is $274 \pm 1^\circ\text{K}$.

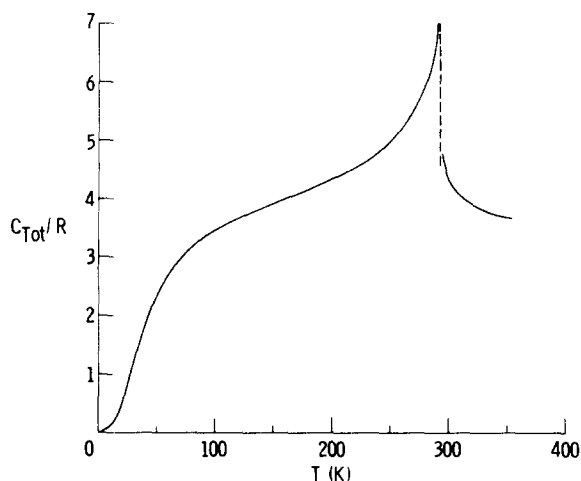


FIG. 2. Total heat capacity at zero field of Gd as a function of temperature (data from Ref. 16).

data and new experimental data. Then, various thermal cycles are examined to show which one can best utilize the accessible area in the entropy-temperature plane. The ideas developed can clearly be applied to both heat pumps and heat engines and to other temperature ranges.

SIMPLE PROCESS ΔT AND ΔS FOR A FERROMAGNET

The reversible temperature rise ΔT in an adiabatically isolated 50-g sample of Gd, initially at 1°C, caused by applying a magnetic field, is shown in Fig. 1. (The sample was a polycrystalline cast cylinder with length/diameter=5 and slightly irregular ends. The temperature at the center of the sample was measured with a copper-constantan thermocouple.) Clearly, this reversible temperature change (also known as the magnetocaloric effect) of about 9°K for a 7-T applied field is large enough to be observed easily and might be useful in some application. It is not, however, large enough to be useful in a heat-pump or an air-conditioning application, as will be shown by considering an entropy-temperature (S - T) diagram for Gd.

It is convenient to construct the S - T diagram from heat capacity and magnetocaloric-effect measurements. The measured total heat capacity C_{Tot} of Gd¹⁶ (shown in Fig. 2) can be integrated, as discussed in Appendix A, to give the entropy as a function of temperature in zero applied magnetic field. Measurements of the reversible adiabatic temperature rise caused by applying a 7-T field are plotted in Fig. 3 as a function of the initial temperature. The effect was reversible to within the experimental error. The high electrical resistivity of Gd in the neighborhood of the Curie point favors a low value of eddy current heating. In Fig. 4, the zero-field entropy curve is plotted, and from it and the results of Fig. 3, the 7-T entropy curve can be obtained. For each temperature on the zero-field curve, the appropriate temperature rise (from Fig. 3) is added to give the temperature on the 7-T curve at the same entropy.

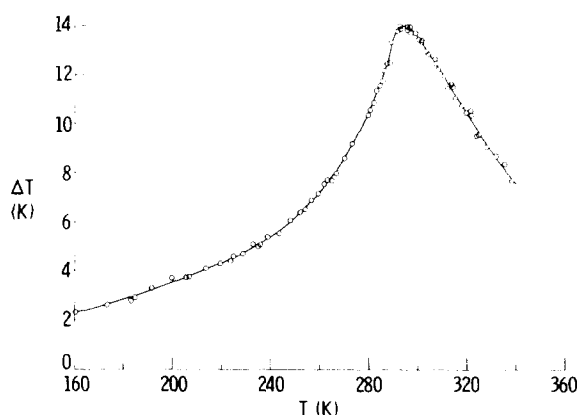


FIG. 3. Reversible adiabatic temperature rise ΔT produced by applying a 7-T field as a function of initial temperature T .

Consider now the simple processes from which a closed thermodynamic cycle could be constructed. An isothermal magnetization can be performed by enforcing good thermal contact between the magnetic substance and a heat sink during the increase in field. The system, therefore, follows a path such as AB in Fig. 4. It is noteworthy that this isothermal process is possible in the magnetic system. The analogous process in a gas-dynamic cycle, isothermal compression, can be approached only by employing several stages of adiabatic compression with intercooling.

From point B, an adiabatic demagnetization process carries the system along the horizontal line to point C and, in this case, covers a temperature range of only about 10°K. A closed cycle could be completed by demagnetizing adiabatically only to point D, demagnetizing to zero field isothermally along D → E, and finally magnetizing adiabatically along E → F. The complete cycle FBDEF is a Carnot cycle. The illustrated cycle spans a temperature range of only 5°K, a span perhaps too small to be of interest without staging. The entropy pumped per cycle is 0.096R. For comparison, the isothermal entropy change produced at various tem-

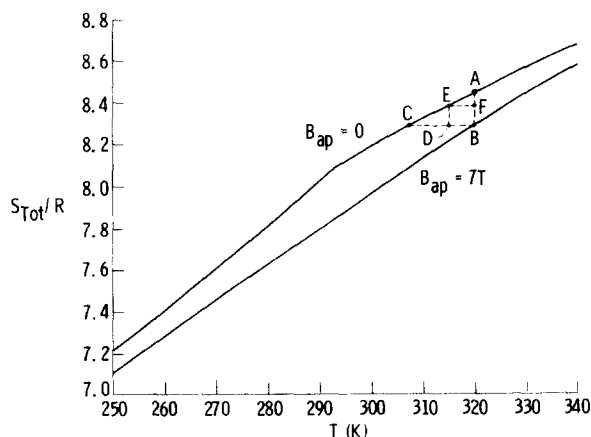


FIG. 4. Total entropy S_{Tot} of Gd as a function of temperature T for applied fields B_{ap} of zero and 7 T.

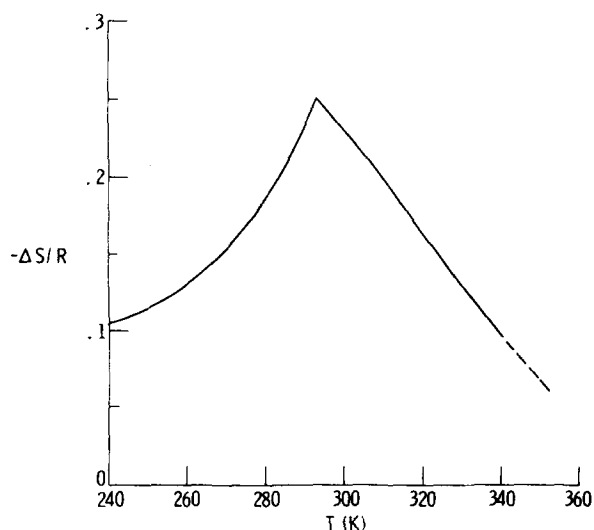


FIG. 5. Isothermal entropy change produced by application of a 7-T field.

peratures by applying a 7-T magnetic field (derived from Fig. 4) is shown in Fig. 5.

It is obvious that the entropy pumped per cycle ΔS and the temperature span ΔT are severely restricted because the cycle is confined between two constant field curves which have positive slopes, whereas the cycle contains two horizontal adiabats. This problem is made more vivid if the processes are plotted in terms of the magnetic entropy S_M rather than the total entropy S_{Tot} :

$$S_M = S_{Tot} - S_L - S_E,$$

where S_L is the lattice entropy and S_E is the conduction-electron entropy. The lattice and conduction-electron entropies can be calculated as a function of temperature, as discussed in Appendix A. If their sum (which is nearly independent of magnetic field) is subtracted from the total entropies plotted in Fig. 4, the magnetic entropy curves of Fig. 6 are obtained and the cycle can be plotted in terms of the active part of the system only. The adiabat BC in Fig. 4 becomes a line with a sharp negative slope in Fig. 6. This is because, at constant total entropy, the entropies given up by the lattice and conduction electrons are absorbed by the magnetic-moment system. The cycle FBDEF is seen to be a very poor utilization of the available S - T space between the constant field curves. Clearly, a different process is needed to connect the sink and source isotherms—a process that does not have the severe negative slope of the total-system adiabat.

REMOVAL OF THE LATTICE AND ELECTRONIC LOAD

A magnetic-moment system unencumbered by other heat capacities would adiabatically demagnetize at constant magnetic entropy as, for example, along $B \rightarrow G$ in Fig. 6. That process spans 35°K, compared to only 13°K for the process $B \rightarrow C$. van Geuns¹ proposed a 4 to 15°K paramagnetic cycle in which the lattice load was removed from the spin system by a regenerator. If an appropriate temperature gradient is

set up in a regenerator material (supercritical helium in van Geuns's case) and if the field strength is varied in an appropriate way, then the heat discharged by the lattice in cooling and the corresponding heat needed in warming can be stored in and withdrawn from the regenerator. The warming and cooling processes are then such that the magnetic entropy and hence the magnetization are constant.

A constant magnetization process, like that of van Geuns, can clearly be done on a ferromagnetic material at room temperature also. A rectangular cycle in the S_M - T plane is the result and such a cycle is shown in Fig. 6 as BLJKB. The possible temperature span ΔT of that cycle is much greater than that of the simple (lattice-loaded) cycle BDEFB. Alternatively, for the same ΔT , the entropy pumped ΔS would be larger. There is an obvious trade-off between ΔS and ΔT . The maximum ΔT 's for the two cycles as a function of the sink temperature T_s are plotted in Fig. 7 for a 7-T maximum field. The maximum ΔS has already been presented in Fig. 5.

A maximum temperature span of about 46°K is possible for a sink at 340°K. At lower temperatures more appropriate for heat-pump and air-conditioning cycles (sinks at approximately 300–320°K), the ΔT is marginal. With a cascaded system (two or more stages) the ΔT would be more than enough and this kind of cycle might indeed be feasible.

CONSTANT FIELD PROCESS

In a constant magnetization process, the regenerator cools and heats the lattice, but the magnetocaloric effect cools and heats the spin system. If the regenerator

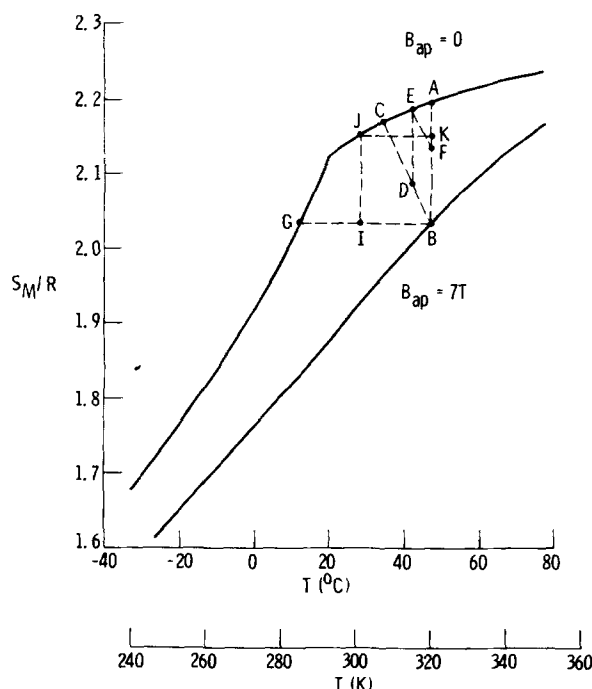


FIG. 6. Magnetic entropy S_M of Gd as a function of temperature T for two applied field strengths B_{ap} .

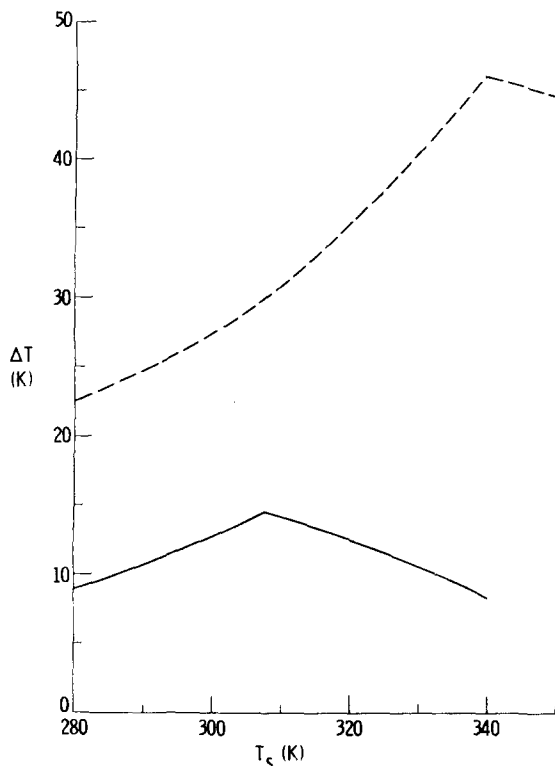


FIG. 7. Maximum temperature span ΔT of a cycle as a function of sink temperature T_s . Solid line—simple cycle, dashed line—"constant magnetization" cycle.

cooled and heated the spin system, too, the entire magnetic effect would be available for isothermal heat absorption or rejection. This can be achieved simply by passing the working material through the regenerator at a constant field rather than at a constant magnetization. A cycle of this type, which will be called a magnetic Stirling cycle because of its similarity to the gas Stirling cycle, is plotted in Fig. 8 as ABLMNA. Two advantages over the previous cycle are obvious. First, the entropy pumped per cycle is increased. But more significantly, the temperature range is not limited by the constraints of the previous two cases.

Figure 9 presents a very simple way of realizing this cycle as a refrigerator, for the sake of definiteness. The regenerator is a vertical column of fluid and the magnetic working material is immersed in it. The fine division of the magnetic material (by granulation, porosity, lamination with gaps for fluid flow-through, etc.) enhances thermal contact with the regenerator fluid (at the expense of some reduction of packing density of the magnetic material). A heat transfer coil to remove the heat of magnetization is indicated schematically at the top and a coil is at the bottom to represent the thermal load.

Starting the refrigerator begins with isothermal magnetization of the working material at the top. Then, at constant field, the working material is moved to the bottom of the regenerator. (Clearly, it is equivalent to move the regenerator tube upward). The field is then reduced and the cooling occurs. As the working material passes back through the regenerator, the "cold" is

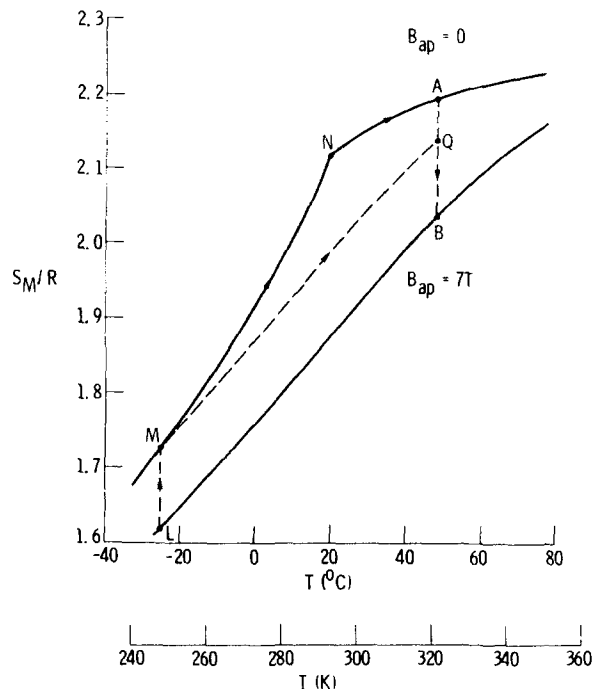


FIG. 8. The magnetic Stirling cycle QBLMQ plotted in the magnetic entropy-temperature plane.

transferred, setting up a temperature gradient in the regenerator. After another isothermal magnetization at the top and another transit (at constant field) through the regenerator, the working material arrives at the bottom colder than before. Demagnetization then produces a new lower temperature and the regenerator is further cooled by raising the working material to the top. Additional cycles build up the regenerator temperature gradient and reduce the temperature of the

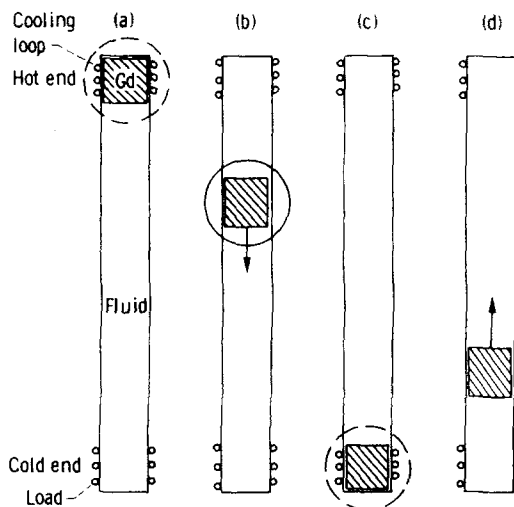


FIG. 9. Magnetic Stirling cycle. Solid circle represents field on. Dotted circle in (a) represents field increasing; in (c), field decreasing. The processes are (a) isothermal magnetization, (b) constant field cooling in regenerator, (c) isothermal demagnetization, and (d) zero (or low) field heating in regenerator.

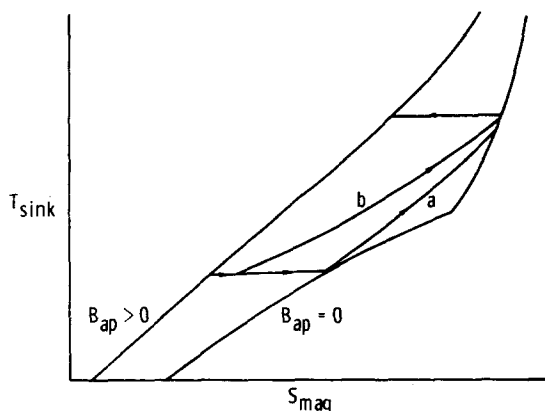


FIG. 10. Comparison of cycles with isothermal heat loads and (a) no other heat load, (b) a heat load distributed over a temperature range.

cold end of the regenerator. Lower and lower temperatures will be produced until losses consume the entire cooling effect or until the bottom heat transfer loop is connected to a heat load. A vertical regenerator orientation with the cold end down is chosen to maximize stratification and thus to minimize mixing of the regenerator fluid.

There are two important points to emphasize about the regenerator. One is that the cooling effect of demagnetization is cumulated cycle after cycle in the regenerator. The other is that once the regenerator thermal gradient is established, it does the entire job (except for making up losses) of carrying the lattice and the magnetic system between the sink and source temperatures. Unfortunately, for maximum efficiency the warming and cooling processes cannot both be constant field processes. This can be seen by considering the cycle as plotted in Fig. 8 and noting that the bounding constant field lines are not the same shape. This gives rise to a problem similar to one that occurs with a nonideal gas in a counterflow heat exchanger in which the heat capacities of the two streams are not equal at all temperatures. In the magnetic system, the magnetic heat capacities at constant applied field are not equal at different field strengths, which would lead to regenerator heat transfer losses. Another aspect of the same problem is that the isothermal entropy changes at an arbitrarily chosen pair of sink and source temperatures are not generally the same. A cycle with Carnot efficiency must reject the same amount of entropy to the sink that it absorbs from the source.

In the magnetic system, the applied field offers a degree of freedom that can overcome the above entropy balance problems. Such freedom does not exist in the gas-refrigeration system because the analogous variable is pressure. Pressure cannot be varied at will along a flow process and, in a batch process, it is awkward to maintain thermal contact with the gas because the volume changes with temperature and pressure. In the magnetic cycle, the process MNA in Fig. 8 can be replaced by the process MQ (drawn parallel to LB) by an appropriate variation of the applied magnetic field during the warming process. The entropy changes can

thereby be balanced. Obviously, either one or both legs of the cycle can be so modified. An appropriate programming of the field during regeneration should be possible and practical. Work is done on the external system by the magnetic material during some of these field changes and the associated energy must not be wasted if Carnot efficiency is to be obtained.

The magnetic refrigerator can, in principle, handle a load (e.g., a sensible heat load) distributed over a range of temperatures with the maximum theoretical efficiency (that is, with the same work as required by an array of infinitesimal Carnot refrigerators, each working between the sink temperature and an increment of the distributed temperature of the load.) For example, a liquefier which must cool incoming gas to the condensation point has this kind of load in addition to the isothermal latent heat load. The distributed load can be absorbed in the regenerative magnetic cycle by a programmed demagnetization during the leg of the cycle where the magnetic material's temperature rises. Thus, more heat is absorbed in the warming leg than was rejected during the cooling leg. Such a cycle is sketched on the T - S diagram for Gd in Fig. 10 for a combination of isothermal and distributed loads. (Note the reversal of the T and S axes from previous plots.) In practice, it may be difficult to obtain good thermal contact between the magnetic working material and the distributed load. One simple approach for cooling a gas would be to pass the gas downward in thermal contact with the regenerator column, for example, coaxially or through a tube attached to the outside of the regenerator column.

The introduction of Stirling-like regeneration expands the temperature range of the magnetic cycle to such an extent that the existing data do not suggest any clear temperature limit. A glance at Fig. 8 suggests that the temperature range may perhaps be expanded to 100°K or more.

At this writing, a temperature span of 47°K has been achieved in a simple device. The experimental arrangement was essentially that shown in Fig. 9 but without any load or cooling loop. One mole of 1-mm-thick Gd plates, separated by screen wire to allow the regenerator fluid to pass through in the vertical direction, was arranged in a cylindrical assembly. This assembly was held stationary in a water-cooled electromagnet. The tube containing the regenerator fluid (400 cm³ of 80% water and 20% ethyl alcohol) was oscillated up and down and the 7-T field was turned on and off at appropriate times during the cycle, as previously described. The regenerator fluid was initially at room temperature, but after about 50 cycles the temperature at the top reached 46°C and the temperature at the bottom reached -1°C. Because of the absence of a load and a heat sink, the cycle was not operating between strict isotherms. Nevertheless, this test demonstrates that the regenerative cycle can produce a temperature span much greater than the nonregenerative cycles. There were substantial losses in the regenerator due to imperfect sealing around the moving element and due to liquid jets which produced mixing in the regenerator. Proper design of the moving element

should minimize these losses and further increase the temperature span. Measurements of efficiency are planned.

Regenerator losses will undoubtedly limit the maximum temperature span as well as the cycle efficiency, but the analysis of these and other losses is outside the scope of this paper. Below the Curie point, magnetic hysteresis losses may appear at low field because of the formation of domains with various orientations of the magnetization. This could be minimized by various means such as reducing the demagnetizing factor of the piece of working material, using single crystals with appropriate "easy" axes, selecting an appropriate particle size as is done with permanent magnet materials, etc. Another problem which occurs in gadolinium, even in oriented single crystals, is the temperature-dependent deviation of the spontaneous magnetization away from the *c* axis below about 240 °K.¹⁷

With the expansion of the temperature range ΔT , the possible isothermal entropy change ΔS at one or both isotherms will be substantially smaller than near the Curie point, as shown in Fig. 5. (Below the Curie point, the spontaneous magnetization decreases the possible entropy change. Above the Curie point, the applied field is less effective because of thermal disordering and because the aiding internal Weiss field is smaller.) To circumvent this decrease in ΔS and to achieve even greater ΔT , staging can be considered. The concept is straightforward; the heat sink for a low-temperature stage is the source of the higher-temperature stage.

WORKING SUBSTANCE

It is shown in Appendix B that, for magnetic materials with the same Curie point magnetothermal effects depend quadratically on gJ , where g is the spectroscopic splitting factor and J is the total magnetic-moment quantum number. The rare earths with high J are thus preferred over the transition elements. (Moreover, transition elements must be diluted in order to bring the Curie point down to room temperature.) Gadolinium has the highest Curie point (293 °K) of the ferromagnetic rare-earth elements and is the only pure rare earth suitable for use near room temperature. It has a half-filled *f* shell which has no net orbital angular momentum and, therefore, the crystal field effects are minimized. The entire free-atom degeneracy of $2J + 1 = 8$ energy levels is preserved in the metal, which is important since the maximum magnetic entropy is $R \log(2J + 1)$.

Intermetallic compounds and alloys of Gd or other rare earths allow an optimum choice of the Curie temperature for any desired range of operating temperatures. Table I presents a few examples, taken from Ref. 18, of compounds with Curie points ranging from 24 to 336 °K. There are also alloys and compounds of the transition metals which have Curie points in the room-temperature range and lower, and their lower cost would be an advantage. Whether the lower cost would compensate for the decreased performance due to the smaller J is unanswerable without a detailed engineering analysis of the cycle.

COMPARISON WITH GAS CYCLE

Some fundamental comparisons of the magnetic cycles with gas cycles are interesting. Consider first the isothermal entropy change that can be effected. In Gd, this is of the order of $0.2R$ near the Curie point for the 7-T magnetic field used in this study. In a gas far from its boiling point, the entropy change is R times the natural log of the pressure ratio. Pressure ratios might range from 3 to 100, giving corresponding molar entropy changes of $(1-5)R$, which is 5-25 times that of Gd. Thus, on a molar basis, the entropy change of the gas looks much better. On a volume basis, however, the magnetic material fares much better because its density is much higher and constant—an engineering convenience. The molar volume of low-pressure gas (STP) is 22 400 cm³, compared to 20 cm³ for Gd; i. e., the molar density of Gd is 1000 times that of STP gas. Hence, the volumetric entropy change is 40-200 times greater than that of gas, based on the uncompressed gas volume. If the low-pressure stream in the gas case is at 10 atm (to reduce the molar volume), a reasonable pressure ratio is 10, giving a gas entropy change of $2.3R$. Hence, Gd is still better by a factor of 90 in entropy change per volume. Thus the magnetic refrigerator might be rather compact depending, of course, on the sizes of the magnet and other components.

A less optimistic comparison can be made in terms of the ratio of useful heat pumped per cycle to the amount of heat transferred to and from the regenerator per cycle. This quantity is expected to be related to losses in a real device so it is of interest to compare the values in a regenerative magnetic cycle to those in a regenerative or counterflow-heat-exchanged gas cycle. The amount of heat removed from the working material in cooling from sink to source temperature is proportional to the average heat capacity and to the temperature span. The ideal gas heat capacity C_p is $2.5R$ for a monatomic gas such as helium, whereas, above the Debye temperature, the lattice heat capacity of a solid approaches $3R$. The magnetic heat capacity,

TABLE I. Examples of ferromagnetic rare-earth intermetallic compounds (data taken from Ref. 18). The asterisk denotes T_c at 19 kOe.

Compound	Curie temperature (°K)	Saturation moment per R. E. atom at 4 °K, Bohr magnetons
Gd ₅ Si ₄	336	7.2
Gd	293	7.5
Gd ₃ Al ₂	282	7.1
Tb ₅ Si ₄	225	6.5
Gd ₃ In	213	5.2
GdAl _{1.9} Ni _{0.1}	191	7.2
GdAl ₂	182*	7.1
Tb _{0.2} Gd _{0.8} Al ₂	168*	7.4
Dy ₅ Si ₄	140	7.1
TbAl ₂	121*	8.6
Tb _{0.8} Dy _{0.2} Al ₂	109	8.5
Ho ₅ Si ₄	76	7.4
DyAl ₂	70	9.6
HoAl ₂	42*	9.2
ErAl ₂	24*	7.0

which for Gd is as high as $4R$ but typically of order R , must be added to the latter figure. Thus, in any unit temperature span, the regenerator must store and resupply an average of about $4R$ in the magnetic case compared to $2.5R$ in the gas case, but the useful product (heat pumped per mole per cycle) is only $0.2-0.04$ as much. Thus the magnetic cycle is likely to be much more sensitive to regenerator losses. The fact that neither the working substance nor the regenerator fluid changes density during the cycle and that the fluid is a dense liquid rather than a gas may permit efficient heat transfer design and offset the apparent disadvantage. Also, as mentioned previously, the heat capacities of warming and cooling working material can be equalized in the magnetic case. Further, the advantage of isothermal magnetization lies with the magnetic system because isothermal compression is not convenient in the gas system.

CONCLUSIONS

Magnetothermal effects have been shown to be large enough for practical use at room temperature if a suitable material is chosen. A ferromagnetic material is required with its Curie point in or near the temperature range of the cycle. To span a reasonable temperature difference and to pump as much entropy per cycle as possible, the load of the lattice and the electronic heat capacities can be lifted off the magnetic system by a regeneration technique. A worthwhile increase in the cycle ΔT is obtained in the constant magnetization cycle. But a much greater increase in ΔT is possible in the magnetic Stirling cycle which uses constant (or nearly constant) applied field during regeneration. The efficiency of all of the cycles discussed is, in principle, the ideal Carnot efficiency. Isothermal heat rejection is possible in the magnetic cycle, which is noteworthy because isothermal compression is not feasible in practice with a gas. The heat capacities of the magnetic working material can be equalized in the warming and cooling processes by magnetic field control. Field control also permits the refrigerator to accept a heat load that is distributed over a range of temperatures without a reduction in efficiency. The techniques that have been described are applicable to engines as well as heat pumps.

APPENDIX A. ZERO-FIELD ENTROPY OF Gd.

Heat capacity and entropy are related by $C dT = T dS$, so one can use

$$S - S_0 = \int_{T_0}^T \frac{C dT}{T} \quad (\text{A1})$$

to calculate entropy as a function of temperature when $C(T)$ is known. We take $T_0 = 0$ and $S_0 = 0$. Equation (1) was used to calculate the total entropy S_{Tot} at zero field from the known experimental heat capacity.¹⁶ The result is plotted in Fig. 4.

The lattice entropy S_L and the conduction-electron entropy S_E may be found in the same way from the corresponding heat capacities. The lattice heat capacity C_L is calculated from the Debye model with the Debye

temperature θ_0 taken as 172°K (a value near that from sound velocity results):¹⁴

$$C_L = 9R \left(\frac{T}{\theta_0} \right)^3 \int_0^{\theta_0/T} \frac{e^x x^4 dx}{(e^x - 1)^2}. \quad (\text{A2})$$

The electronic heat capacity C_E is taken to be

$$C_E = 2.6 \times 10^{-3} \text{ T cal/mole } ^\circ\text{K}, \quad (\text{A3})$$

where the constant 2.6 is the average between the values 2.51 and 2.69 which were measured for La¹⁹ and Lu,²⁰ respectively. The magnetic entropy S_M at zero field is then calculated from

$$S_M = S_{\text{Tot}} - S_L - S_E. \quad (\text{A4})$$

APPENDIX B. INDEPENDENCE OF T_c AND J AND BENEFIT OF LARGE J

In classical molecular field theory, it is rather easily derived that the Curie temperature T_c depends on J and the molecular field coupling-constant K according to

$$T_c = N \mu_B^2 g^2 J(J+1) / 3k,$$

where N is the number of dipoles per unit volume, g is the Lande spectroscopic splitting factor, μ_B is the Bohr magneton, and k is the Boltzmann constant. (See, for example, Ref. 21, pp. 262–268.) Materials can have different values of J yet have the same Curie temperature by having appropriate values of K . For the working material in a magnetic heat pump, one wants to select a suitable Curie point, but one also wants to obtain the maximum response to an externally applied field. The simplest evidence that higher values of J are therefore preferred is furnished by the Curie-Weiss law derived from molecular field theory. This states that for weak applied fields above the Curie point, the magnetic susceptibility χ obeys

$$\chi = Ng^2 \mu_B^2 J(J+1) / 3k(T - \theta),$$

where θ , the paramagnetic Curie temperature, is near, but usually slightly greater than, the ferromagnetic Curie temperature. The coupling constant appears here only indirectly in θ . The quadratic behavior of susceptibility with J leads to a similar behavior of the magnetocaloric effect and makes rare earths much better than transition metals for the present application. A further reason why transition metals are inferior is that, because their d electrons interact very strongly, they have much higher Curie points for equal concentrations than the rare earths. Of course, the Curie point of iron, for example, can be lowered to room temperature by alloying it or putting it into a compound, but this reduces the number of magnetic moments per unit volume and, concomitantly, the amount of cooling or heating power per unit volume of the working material.

¹J.R. van Geuns, Philips Res. Rep. Suppl. 6 (1966).

²G.V. Brown, in *Proceedings of 13th International Congress of Refrigeration* (International Institute of Refrigeration, Washington, D.C., 1971).

³D.J. Flood, in *Magnetism and Magnetic Materials—1973* (Boston), edited by C.D. Graham, Jr. and J.J. Rhyne

- (American Institute of Physics, New York, 1974), pp. 1345–1348.
- ¹D.J. Flood, NASA Tech. Note D-7675, 1974 (unpublished).
- ⁵D.J. Flood, J. Appl. Phys. **45**, 40 (1974).
- ⁶D.J. Flood, Phys. Lett. A **49**, 59 (1974).
- ⁷T. Edison, British Patent 16,709, 1887.
- ⁸N. Tesla, U.S. Patent 428,057, 1890.
- ⁹L. Brillouin and H.P. Iskenderian, Electron. Commun. **25**, 300 (1948).
- ¹⁰E.L. Resler, Jr. and R.E. Rosensweig, AIAA J. **2**, 1418 (1964).
- ¹¹C. Chilowsky, U.S. Patent 2,510,800, 1950.
- ¹²C. Chilowsky, U.S. Patent 2,619,603 1952.
- ¹³C. Chilowsky, U.S. Patent 2,589,775, 1952.
- ¹⁴J. Rhyne, in *Magnetic Properties of Rare Earth Metals*, edited by R.J. Elliott, (Plenum, New York, 1972), pp. 129–185.
- ¹⁵Malcomb P. Sillars, Master's thesis (West Virginia University, 1965 (unpublished)).
- ¹⁶M. Griffel, R.E. Skochdopole, and F.H. Spedding, Phys. Rev. **93**, 657 (1954).
- ¹⁷W.C. Koehler, *Magnetic Properties of Rare Earth Metals*, edited by R.J. Elliott (Plenum, New York, 1972), pp. 81–128.
- ¹⁸W.E. Wallace, *Rare Earth Intermetallics* (Academic, New York, 1973).
- ¹⁹A. Berman, M.W. Zemansky, and H.A. Boorse, Phys. Rev. **109**, 70 (1958).
- ²⁰O.V. Lounasmaa, Phys. Rev. **133**, A219 (1964).
- ²¹A.H. Morrish, *Physical Principles of Magnetism* (Wiley, New York, 1965).